

Relationship of MRI Delayed Contrast Enhancement to Irreversible Injury, Infarct Age, and Contractile Function

Raymond J. Kim, David S. Fieno, Todd B. Parrish, Kathleen Harris, Enn-Ling Chen, Orlando Simonetti, Jeffrey Bundy, J. Paul Finn, Francis J. Klocke and Robert M. Judd

Circulation. 1999;100:1992-2002

doi: 10.1161/01.CIR.100.19.1992

Circulation is published by the American Heart Association, 7272 Greenville Avenue, Dallas, TX 75231

Copyright © 1999 American Heart Association, Inc. All rights reserved.

Print ISSN: 0009-7322. Online ISSN: 1524-4539

The online version of this article, along with updated information and services, is located on the World Wide Web at:

<http://circ.ahajournals.org/content/100/19/1992>

Permissions: Requests for permissions to reproduce figures, tables, or portions of articles originally published in *Circulation* can be obtained via RightsLink, a service of the Copyright Clearance Center, not the Editorial Office. Once the online version of the published article for which permission is being requested is located, click Request Permissions in the middle column of the Web page under Services. Further information about this process is available in the [Permissions and Rights Question and Answer](#) document.

Reprints: Information about reprints can be found online at:
<http://www.lww.com/reprints>

Subscriptions: Information about subscribing to *Circulation* is online at:
<http://circ.ahajournals.org/subscriptions/>

Relationship of MRI Delayed Contrast Enhancement to Irreversible Injury, Infarct Age, and Contractile Function

Raymond J. Kim, MD; David S. Fieno, BS; Todd B. Parrish, PhD; Kathleen Harris, BS; Enn-Ling Chen, PhD; Orlando Simonetti, PhD; Jeffrey Bundy, PhD; J. Paul Finn, MD; Francis J. Klocke, MD; Robert M. Judd, PhD

Background—Contrast MRI enhancement patterns in several pathophysiologies resulting from ischemic myocardial injury are controversial or have not been investigated. We compared contrast enhancement in acute infarction (AI), after severe but reversible ischemic injury (RII), and in chronic infarction.

Methods and Results—In dogs, a large coronary artery was occluded to study AI and/or chronic infarction (n=18), and a second coronary artery was chronically instrumented with a reversible hydraulic occluder and Doppler flowmeter to study RII (n=8). At 3 days after surgery, cine MRI revealed reduced wall thickening in AI ($5\pm 6\%$ versus $33\pm 6\%$ in normal, $P<0.001$). In RII, wall thickening before, during, and after inflation of the occluder for 15 minutes was $35\pm 5\%$, $1\pm 8\%$, and $21\pm 10\%$ and Doppler flow was 19.8 ± 5.3 , 0.2 ± 0.5 , and 56.3 ± 17.7 (peak hyperemia) cm/s, respectively, confirming occlusion, transient ischemia, and reperfusion. Gd-DTPA-enhanced MR images acquired 30 minutes after contrast revealed hyperenhancement of AI ($294\pm 96\%$ of normal, $P<0.001$) but not of RII ($98\pm 6\%$ of normal, $P=NS$). Eight weeks later, the chronically infarcted region again hyperenhanced ($253\pm 54\%$ of normal, n=8, $P<0.001$). High-resolution ($0.5\times 0.5\times 0.5$ mm) ex vivo MRI demonstrated that the spatial extent of hyperenhancement was the same as the spatial extent of myocyte necrosis with and without reperfusion at 1 day ($R=0.99$, $P<0.001$) and 3 days ($R=0.99$, $P<0.001$) and collagenous scar at 8 weeks ($R=0.97$, $P<0.001$).

Conclusions—In the pathophysiologies investigated, contrast MRI distinguishes between reversible and irreversible ischemic injury independent of wall motion and infarct age. (*Circulation*. 1999;100:1992-2002.)

Key Words: magnetic resonance imaging ■ myocardial infarction ■ ischemia

The extent and degree of myocardial injury after an acute ischemic event are strong predictors of patient outcome, and interventions that reduce injury significantly improve prognosis.¹ MRI contrast enhancement observed early (tens of seconds) after contrast is affected by large-artery patency^{2,3} and microvascular obstruction^{4,5} and is thought to relate to perfusion. Delayed enhancement patterns, defined as those appearing more than a few minutes after contrast (eg, >5 minutes), may reflect different physiological information. After acute infarction, hyperenhancement is observed both with⁴⁻¹² and without¹¹⁻¹⁵ reperfusion and predicts prognosis over the next 2 years.¹⁶

The role of contrast-enhanced MRI in evaluating pathophysiologies other than acute infarction is not well established. For example, it is unknown whether delayed hyperenhancement occurs in dysfunctional but viable myocardium or whether hyperenhancement occurs in reversibly injured regions surrounding acute infarcts. Furthermore, there are conflicting reports concerning the utility of contrast MRI

after infarct healing. In this study, we examined delayed contrast enhancement and wall motion after severe but reversible ischemic injury, acute infarction with and without reperfusion, and chronic infarction in chronically instrumented dogs.

Methods

Experimental Preparation

The care and treatment of the eighteen 25- to 30-kg mongrel dogs was in accordance with the "Position of the American Heart Association on Research Animal Use." Animals were premedicated with 1 mL Innovar-Vet IM (0.4 mg/mL fentanyl and 20 mg/mL droperidol) followed by 11 mg/kg brexvalium IV. The animals were then intubated and ventilated with gas anesthesia (halothane). In 8 dogs, the left circumflex (LCx) coronary artery was instrumented with a hydraulic occluder and a 20-MHz Doppler flowmeter for the study of transient ischemia, and the LAD and/or diagonal(s) were permanently ligated to produce infarction (see Figure 1). In all other dogs, a single coronary artery (LAD or LCx) either was permanently ligated to study nonreperfused infarction (n=6) or was transiently occluded for 90 minutes to study reperfused infarction (n=4).

Received March 9, 1999; revision received June 15, 1999; accepted June 22, 1999.

From Northwestern University Medical School Feinberg Cardiovascular Research Institute (R.J.K., D.S.F., T.B.P., K.H., E.-L.C., J.P.F., F.J.K., R.M.J.), Departments of Medicine (R.J.K., F.J.K.), Radiology (T.B.P., J.P.F.), and Biomedical Engineering (D.S.F., F.J.K., R.M.J.), and Siemens Medical Systems (O.S., J.B.), Chicago, Ill.

Correspondence to Robert M. Judd, PhD, Feinberg Cardiovascular Research Institute, Northwestern University Medical School, 303 E Chicago Ave, Tarry 12-723, Chicago, IL 60611-3008. E-mail rjudd@nwu.edu

© 1999 American Heart Association, Inc.

Circulation is available at <http://www.circulationaha.org>

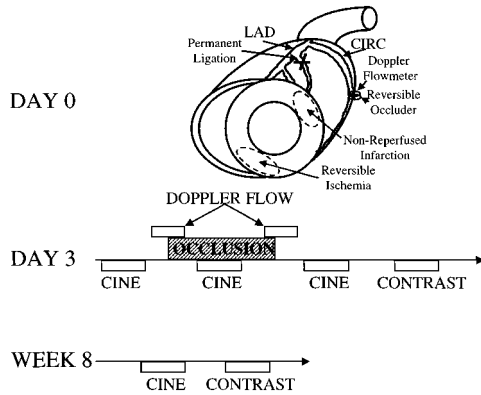


Figure 1. Experimental preparation and MRI protocol.

MRI and Experimental Protocol

Animals were imaged by MRI at 1 day (n=3), 3 days (n=13), and 8 (7.9±0.6) weeks after surgery (n=9). Seven dogs were imaged at both 3 days and 8 weeks.

All animals were anesthetized with sodium pentobarbital 25 mg/kg IV, intubated, and studied on a clinical 1.5-T scanner (Siemens Symphony) in the right lateral decubitus position. A

14×28-cm flexible surface coil was used for imaging. ECG-gated cine MR images encompassing the entire left ventricle were acquired during repeated breath-holds (10 to 15 seconds) to examine wall motion.

In the 8 animals with the reversible occluder, at 3 days after surgery, severe but reversible ischemic injury was produced in the magnet by a 15-minute total occlusion.^{17,18} On the basis of the cine images and knowledge of the intervention, 2 short-axis and 1 long-axis views were chosen as being likely to include the territory distal to the occluder (see Figure 1). Cine MR images of these views were acquired before, during, and after occlusion.

Contrast enhancement was studied after Gd-DTPA 0.3 mmol/kg IV. The agent was injected 30 minutes after release of the occluder, and images were acquired 20 to 30 minutes after Gd-DTPA. T1 weighting was achieved with an inversion-recovery fast low-angle shot (IR-FLASH) pulse sequence. Typical parameters were TE=2 ms, TR=6 ms, voxel size=1×1×6 mm, 300-ms inversion delay, k-space data segmented over 4 cardiac cycles (32 lines per cycle), with data acquired every other cardiac cycle. Images were acquired during breath-hold (≈8 seconds) and were ECG-gated to end diastole.

Ex Vivo MRI and Histology

Hearts from 3 dogs euthanized at 1 day (2 reperused, 1 nonreperused), 4 dogs at 3 days (2 reperused, 2 nonreperused), and 2 dogs

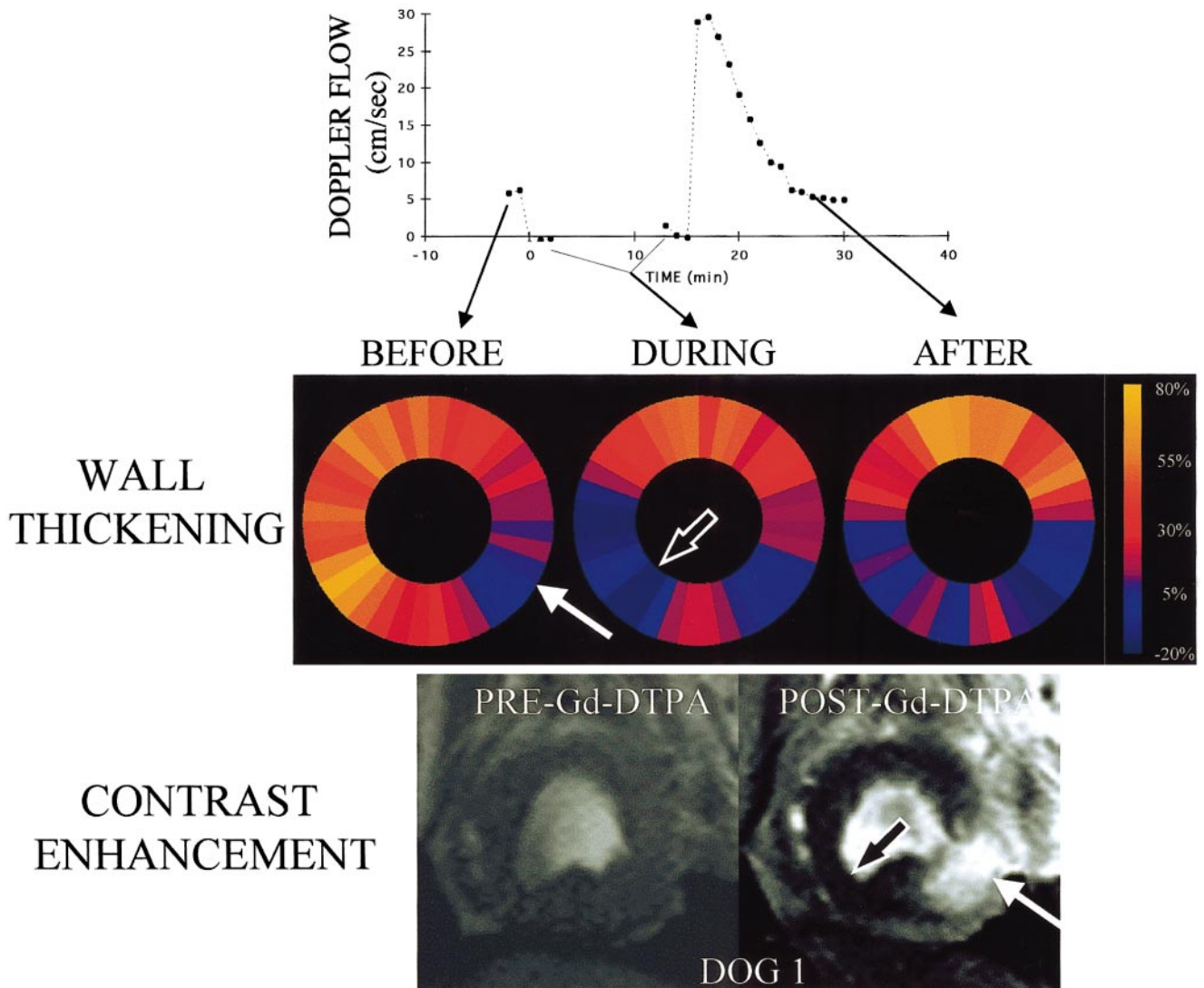


Figure 2. Typical results at 3 days after surgery.

at 8 weeks were subjected to detailed comparison of ex vivo MRI and necrosis defined by triphenyltetrazolium chloride (TTC) over the entire left ventricle. In these animals, the hearts were removed 45 to 60 minutes after Gd-DTPA and quickly rinsed in cold (4°C) saline. To facilitate registration of the ex vivo images, 3 markers were glued to the epicardium near the base. T1-weighted 3D gradient-echo images were acquired with an isometric resolution of 500 μm (TR=20, TE=3.2 ms, flip angle 70°). The hearts were then stiffened by immersion in 95% ethanol precooled to -80°C and sectioned from base to apex into 2-mm-thick short-axis slices with a commercial rotating meat slicer. The cutting plane was defined by use of the 3 markers. All slices were then stained with 2% TTC and photographed. Selected tissue samples were processed for light microscopy (hematoxylin and eosin and/or Masson's trichrome).

Data Analysis

Wall Motion

Wall thickening was determined with commercial software (ARGUS, Siemens) in 36 segments by the modified centerline method.¹⁹

Contrast Enhancement

Image intensities after Gd-DTPA were measured in 3 regions: normal myocardium, myocardium undergoing transient coronary occlusion, and myocardium subtended by permanent coronary occlusion (see Figure 1). These regions were defined on the basis of wall motion. First, the myocardial segment with the worst contractile function was identified in the preocclusion cine MR images. A preliminary normal region was then defined as all segments in the half of the heart opposite the severe contractile abnormality, and the

mean±SD of wall thickening was calculated for this territory. On the basis of these values, the 3 regions were defined as follows: normal region ≡ any group of segments in which wall thickening was within 1 SD of the mean before and during occlusion; transient occlusion region ≡ any group of segments in which wall thickening was within 1 SD of the mean before occlusion but fell below 2 SD of the mean during occlusion; and permanent occlusion region ≡ any group of segments in which wall thickening was <2 SD of the mean before coronary occlusion.

The locations of these regions were then transferred to the post-Gd-DTPA images, and image intensity was measured in the normal region. An observer was then instructed to determine whether hyperenhanced zones, defined as image intensities >2 SD above the mean of the normal region, were present or absent within the transient and permanent occlusion territories. If hyperenhancement was not present, the entire region was outlined. If hyperenhancement was present, the observer thresholded image intensities at a level equal to 2 SD above the mean of the normal region and outlined only the hyperenhancement region to account for nontransmural involvement (see Figures 3 and 4).

Ex Vivo MRI and Histology

For each of the slices stained with TTC, ex vivo images were extracted from the 3D MRI data set. Selection of images was facilitated by the 3 epicardial markers and the uniform slice thickness afforded by the commercial slicer. An independent observer blinded to the MR results analyzed the tissue slices, and a second independent observer blinded to the tissue results analyzed the MR images using the same procedure as described for the in vivo images.

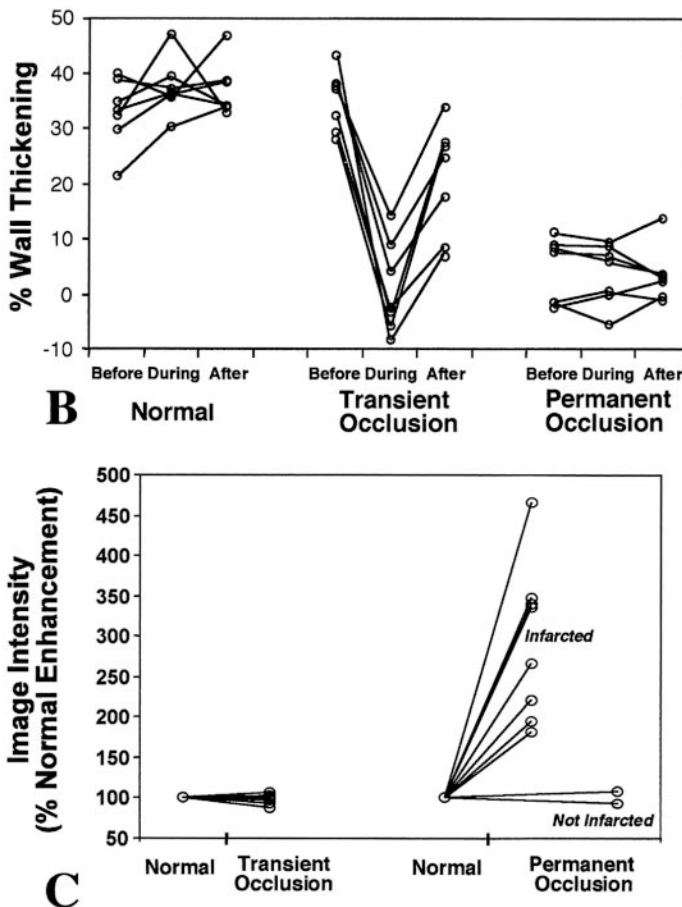
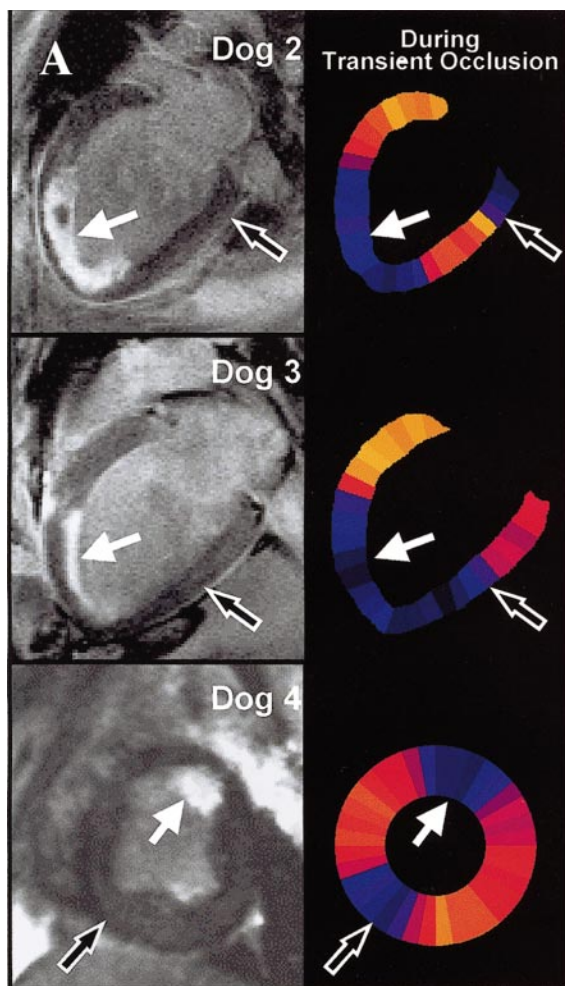


Figure 3. Left, Similar results in 3 additional animals. Right, Wall thickening and image intensities for all animals.

Statistical Analysis

All results were expressed as mean±SD. Wall thickening and image intensity values were compared by 2-factor and single-factor repeated-measures ANOVA, respectively. Bonferroni correction was used for multiple comparisons. All tests were 2-tailed, and a value of $P < 0.05$ was considered significant.

Results

Results at 1 and 3 Days

In vivo enhancement patterns in infarcted regions were similar at 1 and 3 days. Figure 2 compares enhancement patterns in the infarcted region with that of the region subjected to reversible ischemic injury in 1 animal at 3 days after surgery. Before occlusion, cine MRI revealed normal thickening in the LCx territory but reduced thickening in the permanent occlusion territory (3- to 5-o'clock position; LAD diagonal in this animal). During occlusion, verified by the flowmeter (Figure 2, top), cine MRI revealed a dramatic reduction in thickening in the distal LCx territory (6- to 9-o'clock position), confirming that this area became ische-

mic. After reperfusion, wall thickening remained moderately reduced in the transient occlusion territory. Before administration of Gd-DTPA, image intensities in all regions were similar (Figure 2, bottom). After Gd-DTPA, the infarct territory became hyperenhanced, whereas the transient occlusion territory did not become hyperenhanced compared with normal myocardium (10- to 2-o'clock position).

Figure 3A shows similar results in 3 additional animals. In each case, infarcted myocardium became hyperenhanced, whereas myocardial regions after severe transient ischemia with concomitant regional dysfunction did not hyperenhance. Figure 3B summarizes the wall-thickening data at 3 days. In normal regions, thickening remained high before, during, and after transient occlusion ($32.8 \pm 6.2\%$, $37.4 \pm 5.1\%$, and $36.9 \pm 4.9\%$, respectively; $P = \text{NS}$). In the permanent occlusion territory, thickening was significantly lower than normal regions before, during, and after occlusion ($4.5 \pm 5.9\%$, $3.7 \pm 5.5\%$, and $3.5 \pm 4.9\%$, respectively, $P < 0.001$ compared with normal for all times). In the transient occlusion territory,

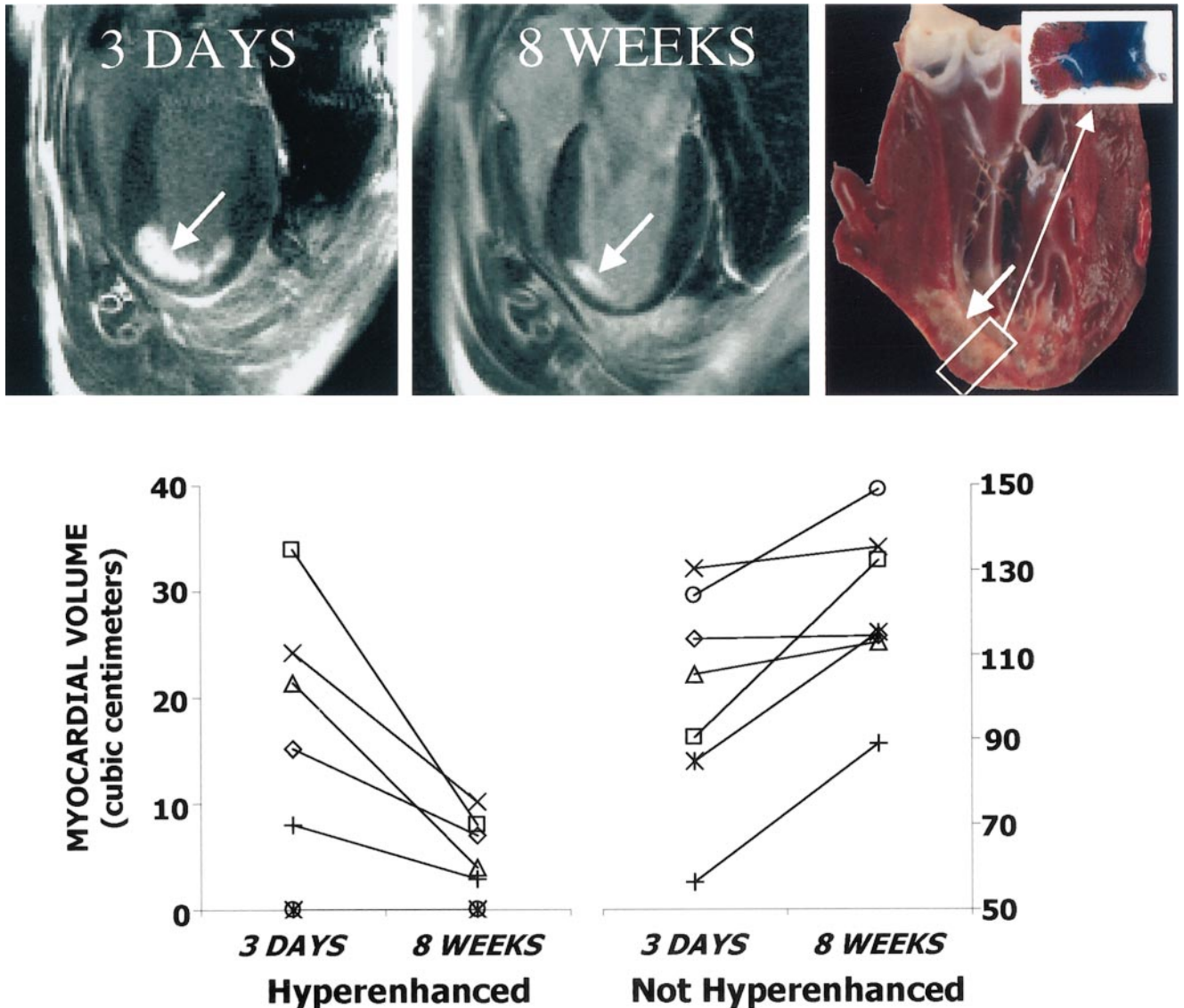


Figure 4. Comparison of results at 3 days and 8 weeks.

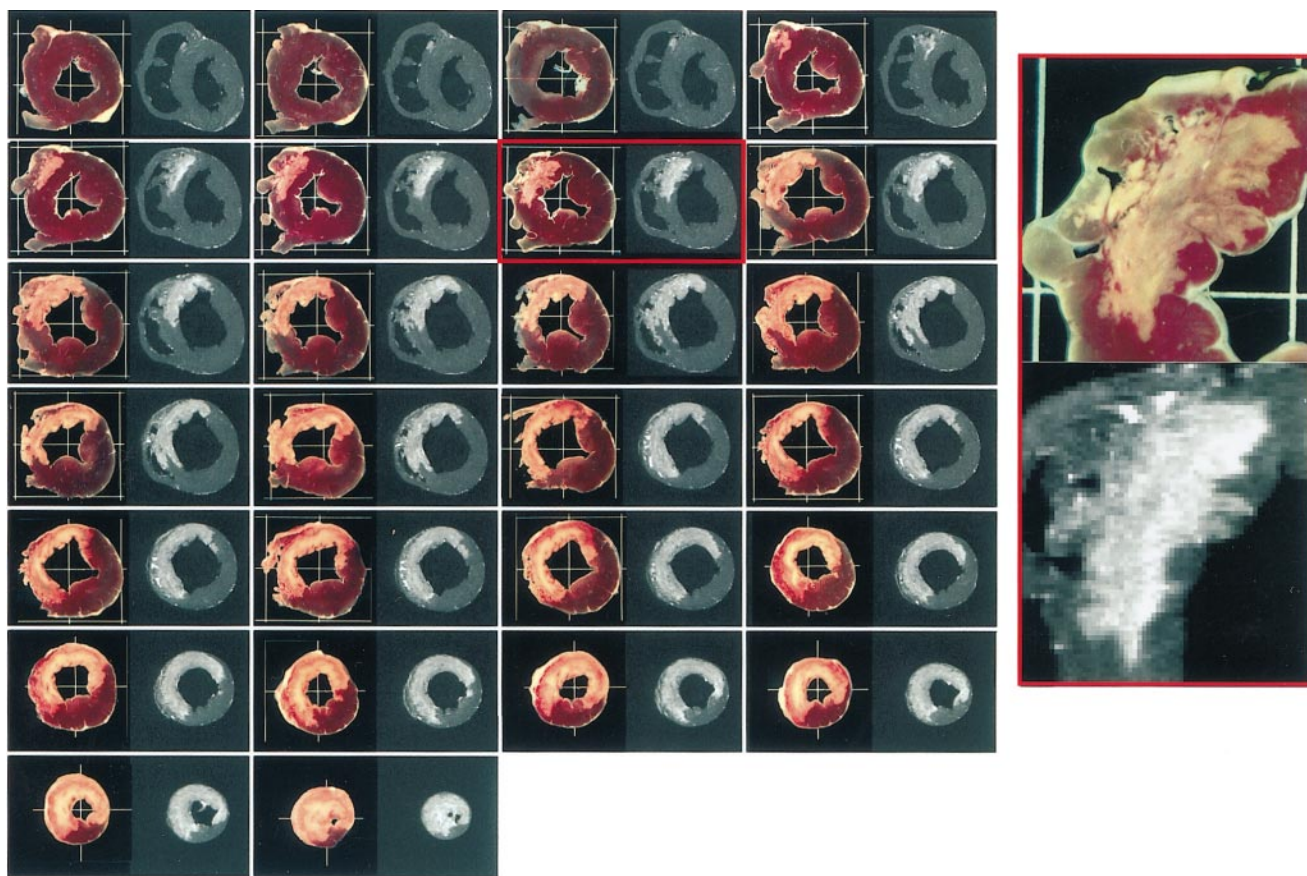


Figure 5. Left, Comparison of ex vivo MR images with TTC-stained slices in 1 animal at 3 days after infarct. Slices are arranged from base to apex starting in upper left and advancing left to right, then top to bottom. Right, Magnified view.

thickening was not different from that of the normal region before occlusion ($35.1 \pm 5.4\%$, $P=NS$) but became significantly lower during occlusion ($1.1 \pm 8.3\%$, $P<0.001$) and remained moderately reduced after reperfusion ($20.9 \pm 10.1\%$, $P<0.001$). Doppler flow before, during, and after occlusion was 19.8 ± 5.3 , 0.2 ± 0.5 , and 56.3 ± 17.7 (peak hyperemia) cm/s, respectively, confirming successful occlusion and reperfusion for all animals. Eight weeks later, wall thickening in the transient occlusion territory returned to baseline levels ($38.7 \pm 5.4\%$, $P=NS$).

Figure 3C summarizes post-Gd-DTPA image intensities at 3 days in the 8 animals subjected to transient occlusion and the 10 animals subjected to permanent occlusion. Image intensities in the transient occlusion territory were the same as those of the normal region ($98.1 \pm 5.7\%$ of normal, $P=NS$). In all animals, no evidence of irreversible injury was found in the region distal to the hydraulic occluder at 8 weeks, confirming that the ischemic injury at 3 days was reversible. Conversely, contrast-enhanced image intensity in the infarcted territory was much higher than in the normal region at 1 day ($506 \pm 51.5\%$ of normal, $P<0.001$) and 3 days ($294.4 \pm 96.1\%$ of normal, $P<0.001$). In all cases, hyperenhancement was easily detected in regions later found to reveal histological evidence of infarction. In 2 animals, the region distal to the permanent occlusion site did not hyperenhance ($101.0 \pm 9.0\%$), and histochemical staining revealed no evidence of infarction.

Results at 8 Weeks

Figure 4, top, shows results in the same animal at 3 days and at 8 weeks. Contrast hyperenhancement is clearly seen after Gd-DTPA administration in both acute and chronic infarction. The photograph of the sectioned heart shows the chronic infarction, which correlated closely in location with the hyperenhanced zone in the MR images. Trichrome staining revealed that the infarct was nontransmural (see inset), and the transmural extent of the scar observed histologically (blue region) appeared to correspond to the transmural extent of the hyperenhanced region in the 8-week MR image. At higher magnification, the trichrome stain revealed that the chronic infarction was a dense collagen matrix.

Figure 4, bottom, summarizes the change in myocardial volume (cm^3) from 3 days to 8 weeks for both the hyperenhanced and nonhyperenhanced regions based on images encompassing the entire left ventricle. Of the 7 dogs imaged at both 3 days and 8 weeks, 2 had no infarction. The absolute volume of the hyperenhanced regions in the remaining 5 dogs decreased by a factor of 3.4 ± 1.4 at 8 weeks compared with 3 days. In all 7 dogs, the absolute volume of the nonhyperenhanced regions increased (1.2 ± 0.2 -fold increase).

Ex Vivo MRI and Histology

Figure 5 compares ex vivo MR images with slices stained with TTC in an animal with a nonreperfused infarct euthanized at 3 days. The location, spatial extent, and 3D shape of

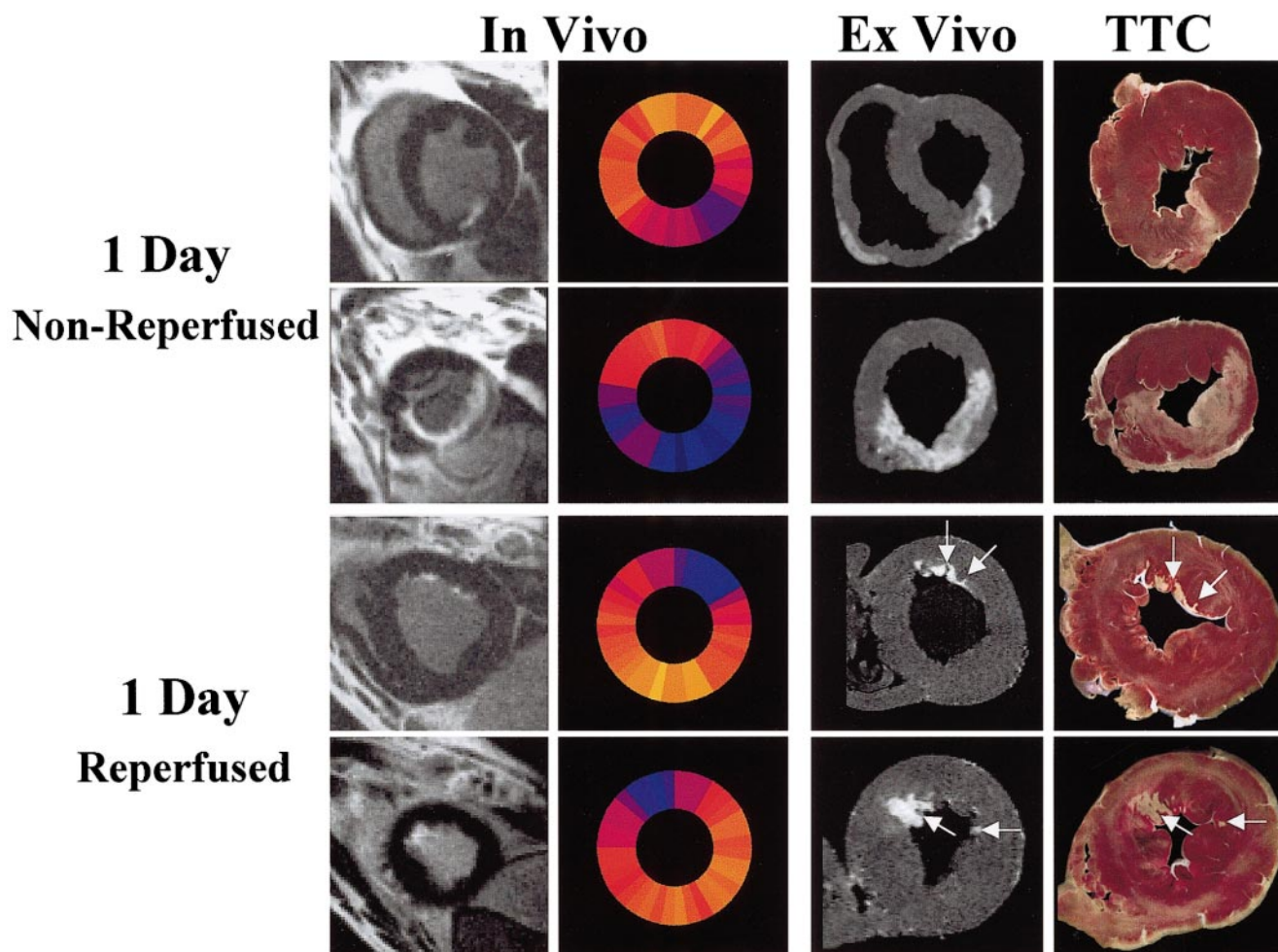


Figure 6. Similar results at 1 day for a nonreperfused infarct in LCx territory (top) and a reperfused infarct in LAD territory (bottom) at midventricular and apical levels. Wall-thickening scale is same as in Figure 2. In reperfused infarct, note that wall thickening was reduced despite predominantly viable myocardium.

the regions of elevated MR image intensity were essentially identical to those of the irreversibly injured regions defined by TTC. Similar results were found in 3-day-old reperfused infarcts. Figure 6 shows similar results at 1 day for both nonreperfused and reperfused infarcts. Figure 7 shows the corresponding results in an animal euthanized at 8 weeks. Despite replacement of the infarct territory with a collagenous scar (verified by light microscopy, see also Figure 4), the regions of elevated MR image intensity were again essentially identical to the irreversibly injured regions defined by TTC. Figure 8 summarizes the results. The regressions were $y=1.02x+0.28$ ($R=0.99$, $SEE=1.97$, $P<0.001$) at 1 day, $y=1.01x+0.59$ ($R=0.99$, $SEE=2.4$, $P<0.001$) at 3 days, and $y=1.03x-0.14$ ($R=0.97$, $SEE=0.76$, $P<0.001$) at 8 weeks.

Figure 9 demonstrates the partial-volume effect. Sixteen consecutive images $500\ \mu\text{m}$ thick were extracted from the 3D MR data set at the location shown in panel A. Hyperenhanced regions had sharp, distinct borders that migrated significantly from slice to slice. Summation of all 16 images resulted in the image in panel B, which has an effective thickness of 8 mm. Intermediate image intensities are introduced along the periphery of the hyperenhancement zone (arrows) due to

partial-volume effects and the complex 3D shape of the infarct.

Discussion

We found that both acute and chronic myocardial infarcts hyperenhance. Myocardial injury without necrosis due to severe, transient ischemia did not lead to hyperenhancement despite the presence of myocardial stunning. The spatial extent of hyperenhancement matched the spatial extent of myocyte necrosis at 1 and 3 days with and without reperfusion and collagenous scar at 8 weeks.

Acute Infarction

Our data are in agreement with previous studies demonstrating that hyperenhancement occurs in both reperfused^{4-7,9-12} and nonreperfused¹¹⁻¹⁵ acute infarcts. However, some reports suggest that hyperenhancement occurs not only in regions of cellular necrosis but also in a border zone of injured but viable myocytes surrounding the acute infarct,^{7,14,20,21} particularly in the first 24 hours. Partial-volume effects may also play a role in the overestimation of infarct size.^{22,23}

The mechanism responsible for hyperenhancement of acutely necrotic myocardium is not clear. Gd-DTPA, with a

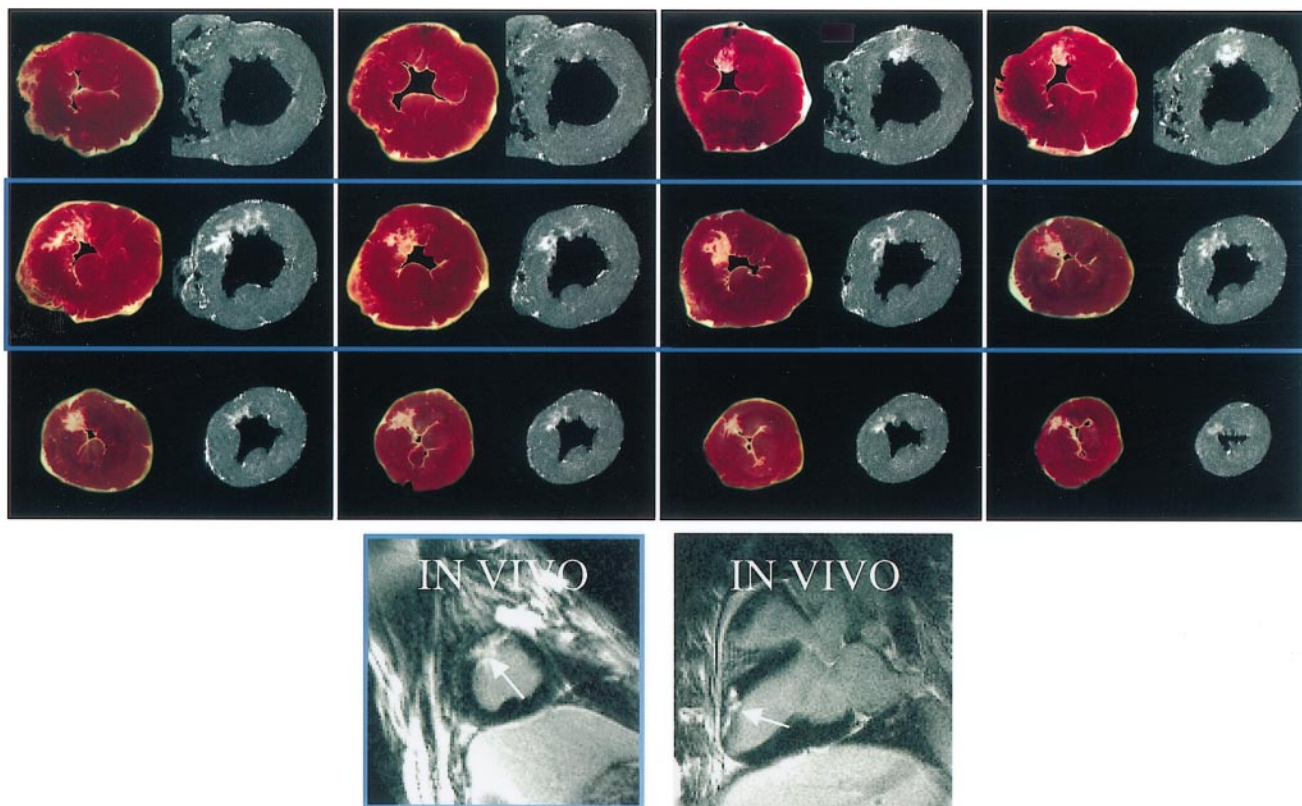


Figure 7. Top, Comparison of ex vivo MR images with corresponding TTC-stained slices in 1 animal at 8 weeks after surgery. Bottom, In vivo images from this animal.

molecular weight of ≈ 800 Da, is thought to be biologically inert and to passively diffuse throughout the extracellular space.²⁴ Other markers of similar molecular weight increase their volume of distribution significantly after myocyte death due to loss of sarcomere membrane integrity.^{25,26} In a previous study of MRI contrast enhancement mechanisms,²³ we reported that regions of hyperenhancement systematically revealed sarcomere membrane rupture examined by electron microscopy. The data also revealed marked changes in

Gd-DTPA wash-in and washout kinetics within the infarct zone compared with normal myocardium. Sarcolemmal rupture, in itself, could affect myocardial Gd-DTPA kinetics, because additional time may be required for contrast molecules to diffuse in and out of isolated breaks in the cellular membrane. Accordingly, it is possible that a physiological event specific for myocyte death, such as myocyte membrane rupture, may relate to the strong correlation between hyperenhancement and acute cellular necrosis.

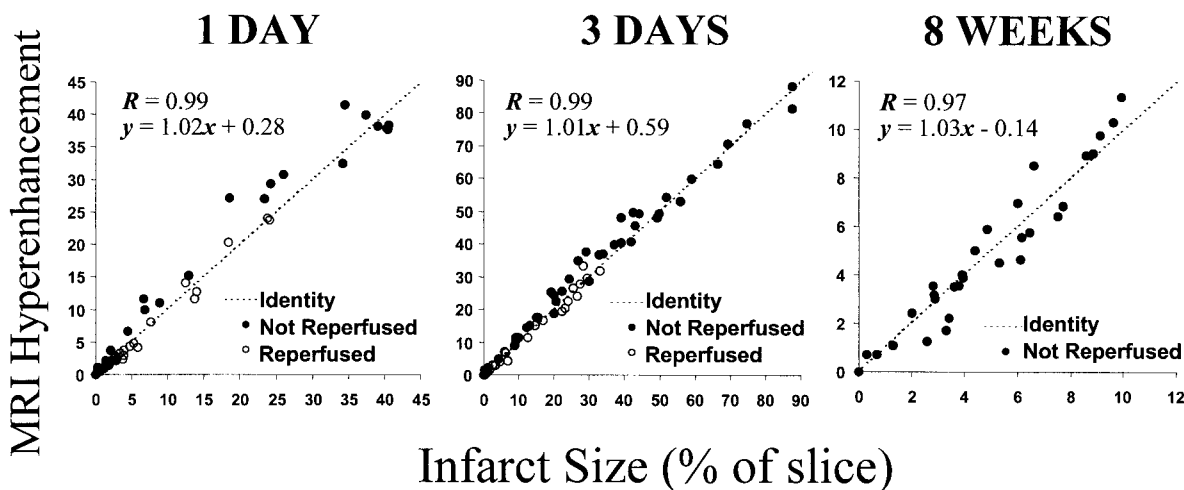


Figure 8. Comparison of hyperenhanced regions with TTC at 1 day (without reperfusion: 1 dog, 21 slices; with reperfusion: 2 dogs, 49 slices), 3 days (without reperfusion: 2 dogs, 50 slices; with reperfusion: 2 dogs, 44 slices), and 8 weeks (without reperfusion: 2 dogs, 59 slices).

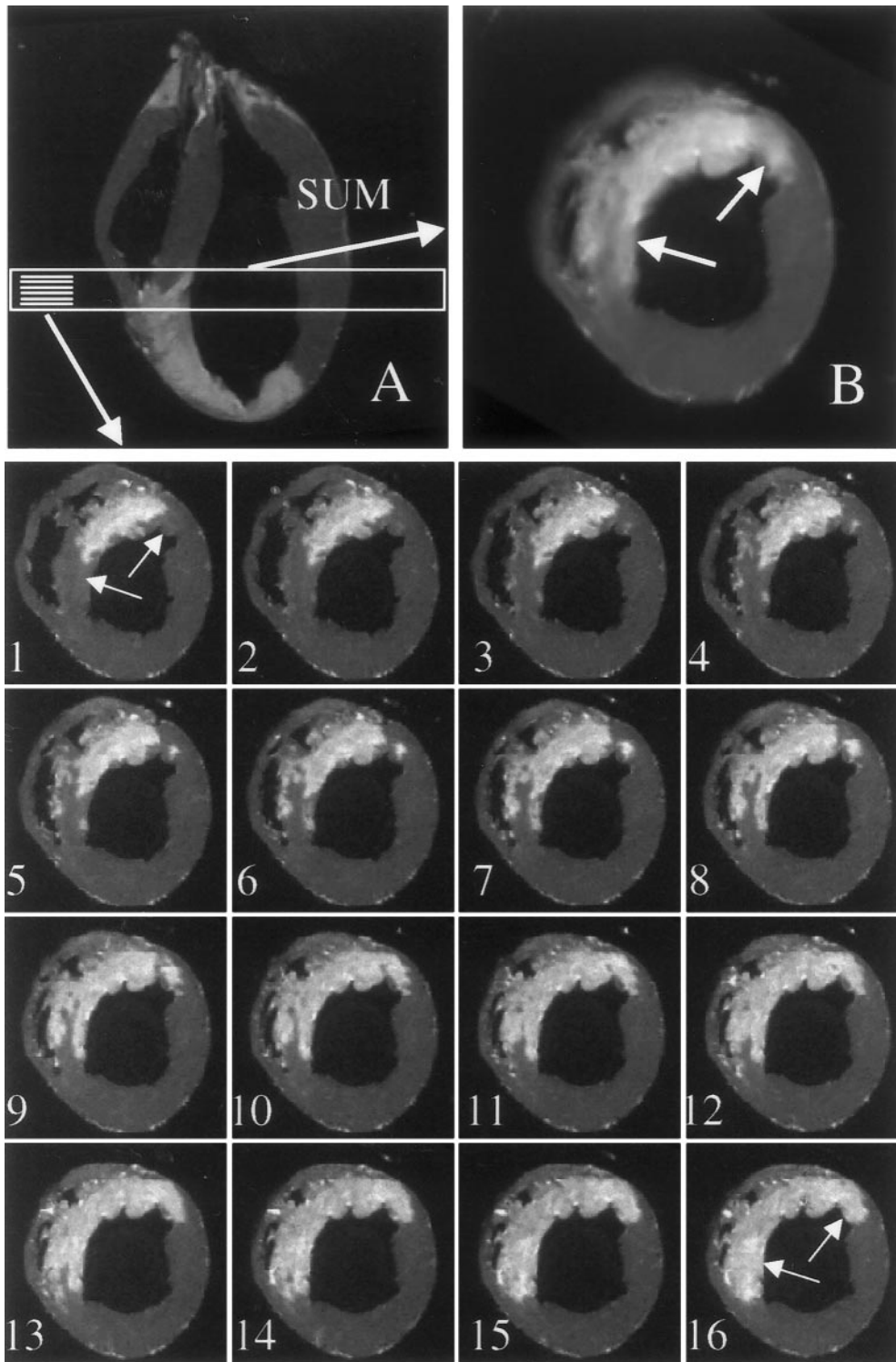


Figure 9. Partial-volume effect.

Chronic Infarction

Contrast enhancement patterns after infarct healing have received less attention than acute infarction. For images acquired more than a few minutes after contrast, some reports suggest that chronic infarcts appear hyperenhanced,^{27,28} but others do not.²⁹⁻³¹ Our data establish that delayed hyperenhancement occurs in nonreperfused myocardial scar. The

mechanism responsible for hyperenhancement of healed infarcts is unknown.

Reversible Ischemic Injury

Whether or not hyperenhancement occurs in injured but viable myocardial regions is controversial. One way to address this question is to examine myocardium subjected to

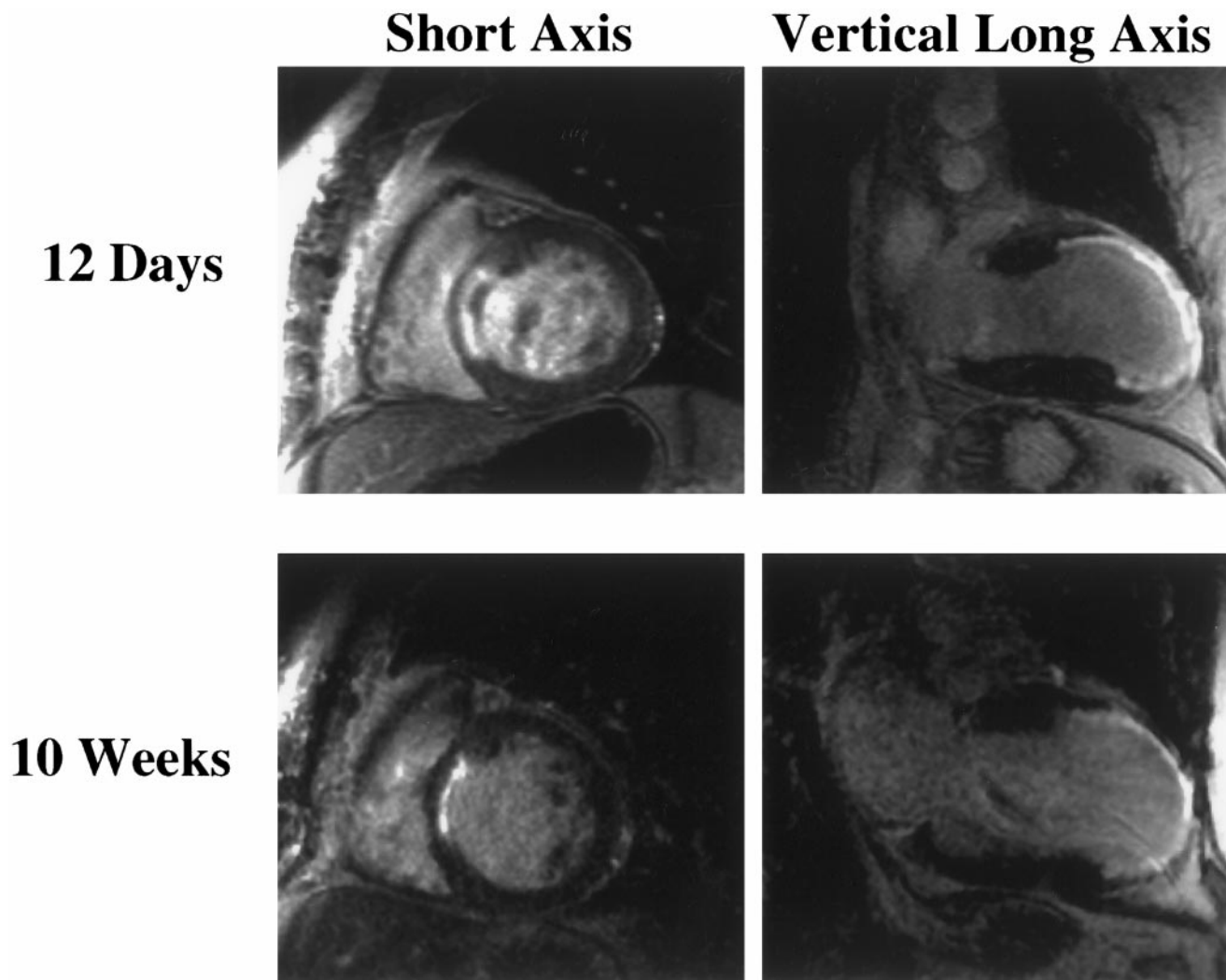


Figure 10. Contrast-enhanced MR images acquired in a patient after a large myocardial infarction in LAD territory. Short-axis images are of basal edge of infarction.

severe but reversible ischemic injury by occluding a canine coronary artery for 15 minutes.^{17,18} McNamara et al⁶ evaluated myocardial contrast enhancement in dogs that underwent 15 minutes of LAD occlusion followed by 24 hours of reperfusion. In agreement with our findings, ex vivo MRI did not show hyperenhancement of the LAD territory.

A related question is whether hyperenhancement occurs in reversibly injured myocardium surrounding regions of myocyte necrosis, particularly in the first week after infarction.^{14,21} Schaefer et al⁷ reported that in the first few hours after infarction, regions of hyperenhancement overestimated infarct size when the contrast agent was injected 5 minutes after reperfusion. Previous studies by our group and others suggest that the spatial extent of hyperenhancement may be similar to that of acute myocyte necrosis.^{5,22,23} Few other studies have directly addressed this issue.

This issue, however, is critical to the interpretation of many MRI observations. In the present study, for example, we found that the absolute volume of hyperenhanced myocardium decreased by a factor of 3.4 between 3 days and 8 weeks (Figure 4). One interpretation of this is that hyperenhance-

ment includes both acutely necrotic regions and surrounding reversibly injured regions at 3 days but that by 8 weeks, the reversibly injured regions have recovered and no longer hyperenhance. Our finding that the spatial extent of hyperenhancement was identical to the spatial extent of myocyte necrosis at 3 days (Figures 5 and 8), however, contradicts this interpretation. Another interpretation of the data of Figure 4 is that the spatial extent of collagenous scar at 8 weeks was 3.4 times smaller than the spatial extent of acute myocyte necrosis at 3 days. Reimer and Jennings report that infarcts shrink \approx 4-fold between 4 days and 6 weeks.^{32,33} Accordingly, the data of the lower left panel of Figure 4 could be explained by infarct shrinkage during the transition from myocyte necrosis to collagenous scar. Extending this concept, the data of the lower right panel of Figure 4 might be explained by compensatory hypertrophy.

Our results also suggest that partial-volume effects should be considered in the interpretation of contrast-enhanced MRI (Figure 9). Whether or not partial-volume effects influenced the results of previous studies is unknown.

On the basis of our findings that hyperenhancement does not occur in purely reversibly injured regions (Figure 3), that

the spatial extent of hyperenhancement is identical to that of acute myocyte necrosis and scar (Figure 8), and that the temporal changes in the spatial extent of hyperenhancement (Figure 4) can be explained by infarct shrinkage,^{32,33} we conclude that hyperenhancement does not occur in reversibly injured regions in the pathophysiologies investigated. Our data do not exclude the possibility of enhancement of a peripheral region surrounding the infarction that resolves by 24 hours.

Clinical Implications

Identification of the spatial extent of viable myocardium is of established clinical importance. Several investigators have reported MRI approaches to identifying viable myocardium, such as wall thickness and dobutamine challenge. Our data suggest a different approach. In the pathophysiologies investigated, the size and shape of regions exhibiting delayed hyperenhancement are identical to regions of irreversible injury. Accordingly, regions that fail to hyperenhance are viable. This finding implies that it is not necessary to consider wall motion in the MRI definition of viability. In fact, the data in Figures 2 and 3 underscore that wall thickening by cine MRI and viability by contrast MRI are dissociated. This dissociation, combined with the ability of contrast MRI to clearly distinguish the transmural extent of acute myocyte necrosis and collagenous scar, suggests that MRI may play an important clinical role in the evaluation of ischemic heart disease. Specifically, our results suggest that contrast MRI in combination with cine MRI might be used in the acute setting to distinguish between acute myocardial infarction (hyperenhanced and with contractile dysfunction), injured but viable myocardium (not hyperenhanced but with contractile dysfunction), and normal myocardium (not hyperenhanced and with normal function). In the setting of chronic coronary artery disease, the combination of contrast and cine MRI may be used similarly to distinguish between myocardial scar, hibernating myocardium, and normal myocardium.

The ability to measure the 3D spatial extent of nonviable and viable myocardium serially over time suggests additional clinical roles. Figure 10 shows contrast-enhanced MR images in a patient 12 days and 10 weeks after a large myocardial infarction in the LAD territory. Similar to the results in Figure 4, this patient showed a reduction in volume of hyperenhanced myocardium (16 mL) along with an increase in the volume of nonhyperenhanced myocardium (34 mL). These results indicate infarct resorption and viable tissue hypertrophy over the 8 weeks between the 2 MRI studies and suggest that contrast MRI may allow noninvasive regional evaluation of ventricular remodeling after ischemic injury with high spatial resolution and full ventricular coverage.

Acknowledgments

This work was supported in part by a Biomedical Engineering Research Grant from the Whitaker Foundation and NIH-NHLBI grant R29-HL-53411 (both to Dr Judd).

References

- Gersh BJ, Anderson JL. Thrombolysis and myocardial salvage: results of clinical trials and the animal paradigm. *Circulation*. 1993;88:296–306.
- Atkinson DJ, Burstein D, Edelman RR. First-pass cardiac perfusion evaluation with ultrafast MR imaging. *Radiology*. 1990;174:757–762.
- Wilke N, Simm C, Zhang J, Ellerman J, Ya X, Merkle H, Path G, Ludemann H, Bache RJ, Ugurbil K. Contrast-enhanced first pass myocardial perfusion imaging. *Magn Reson Med*. 1993;29:485–497.
- Lima JAC, Judd RM, Bazille A, Schulman SP, Atalar E, Zerhouni EA. Regional heterogeneity of human myocardial infarcts demonstrated by contrast-enhanced MRI. *Circulation*. 1995;92:1117–1125.
- Judd RM, Lugo-Olivieri CH, Arai M, Kondo T, Croisille P, Lima JAC, Mohan V, Becker LC, Zerhouni EA. Physiological basis of myocardial contrast enhancement in fast magnetic resonance images of 2-day-old reperfused canine infarcts. *Circulation*. 1995;92:1902–1910.
- McNamara MT, Tscholakoff D, Revel D, Soulen R, Schechtman N, Botvinick E, Higgins CB. Differentiation of reversible and irreversible myocardial injury by MR imaging with and without gadolinium-DTPA. *Radiology*. 1986;158:765–769.
- Schaefer S, Malloy CR, Katz J, Parkey RW, Buja LM, Willerson JT, Peshock RM. Gadolinium-DTPA-enhanced nuclear magnetic resonance imaging of reperfused myocardium. *J Am Coll Cardiol*. 1988;12:1064–1072.
- Saeed M, Wendland MF, Takehara Y, Masui T, Higgins CB. Reperfusion and irreversible myocardial injury. *Radiology*. 1992;182:675–683.
- Peshock RM, Malloy CR, Buja LM, Nunnally RL, Parkey RW, Willerson JT. Magnetic resonance imaging of acute myocardial infarction. *Circulation*. 1986;74:1434–1440.
- Van Rossum AC, Visser FC, Van Eenige MJ, Sprenger M, Valk J, Verheugt FW, Roos JP. Value of gadolinium-diethylene-triamine penta-acetic acid dynamics in magnetic resonance imaging of acute myocardial infarction with occluded and reperfused coronary arteries after thrombolysis. *Am J Cardiol*. 1990;65:845–851.
- van der Wall EE, van Dijkman PRM, de Roos A, Doornbos J, van der Laarse A, Manger Cats V, van Voorthuisen AE, Matheijssen NAA, Brusckhe AVG. Diagnostic significance of gadolinium-DTPA (diethylenetriamine penta-acetic acid) enhanced magnetic resonance imaging in thrombolytic therapy for acute myocardial infarction. *Br Heart J*. 1990;63:12–17.
- de Roos A, van Rossum AC, van der Wall EE, Postema S, Doornbos J, Matheijssen NAA, van Dijkman PRM, Visser FC, van Voorthuisen AE. Reperfused and nonreperfused myocardial infarction. *Radiology*. 1989;172:717–720.
- Rehr RB, Peshock RM, Malloy CR, Keller AM, Parkey RW, Buja LM, Nunnally RL, Willerson JT. Improved in vivo magnetic resonance imaging of acute myocardial infarction after intravenous paramagnetic contrast agent administration. *Am J Cardiol*. 1986;57:864–868.
- Nishimura T, Yamada Y, Hayashi M, Kozuka T, Nakatani T, Noda H, Takano H. Determination of infarct size of acute myocardial infarction in dogs by magnetic resonance imaging and gadolinium-DTPA. *Am J Physiol Imaging*. 1989;4:83–88.
- Wesby GE, Higgins CB, McNamara MT, Engelstad BL, Lipton MJ, Sievers R, Ehman RL, Lovin J, Brasch RC. Effect of gadolinium-DTPA on the magnetic relaxation times of normal and infarcted myocardium. *Radiology*. 1984;153:165–169.
- Wu KC, Zerhouni EA, Judd RM, Lugo-Olivieri CH, Barouch LA, Schulman SP, Blumenthal RS, Lima JAC. Prognostic significance of microvascular obstruction by magnetic resonance imaging in patients with acute myocardial infarction. *Circulation*. 1998;97:765–772.
- Whalen DA Jr, Hamilton DG, Ganote CE, Jennings RB. Effect of a transient period of ischemia on myocardial cells. *Am J Pathol*. 1974;74:381–398.
- Jennings RB, Schaper J, Hill ML, Steenbergen C Jr, Reimer KA. Effect of reperfusion late in the phase of reversible ischemic injury. *Circ Res*. 1985;56:262–278.
- van Rugge FP, van der Wall EE, Spanjersberg SJ, de Roos A, Matheijssen NAA, Zwinderman AH, van Dijkman PRM, Reiber JHC, Brusckhe AVG. Magnetic resonance imaging during dobutamine stress for detection and localization of coronary artery disease. *Circulation*. 1994;90:127–138.
- Masui T, Saeed M, Wendland MF, Higgins CB. Occlusive and reperfused myocardial infarcts: MR imaging differentiation with nonionic Gd-DTPA-BMA. *Radiology*. 1991;181:77–83.
- Baer FM, Theissen P, Schneider CA, Voth E, Schicha H, Sechtem U. Magnetic resonance tomography imaging techniques for diagnosing myocardial vitality. *Herz*. 1994;19:51–64.
- Goldman MR, Brady TJ, Pykett IL, Burt CT, Buonanno FS, Kistler P, Newhouse JH, Hinshaw WS, Pohost GM. Quantification of experimental myocardial infarction using nuclear magnetic resonance imaging and

- paramagnetic ion contrast enhancement in excised canine hearts. *Circulation*. 1982;66:1012–1016.
23. Kim RJ, Chen E-L, Lima JAC, Judd RM. Myocardial Gd-DTPA kinetics determine MRI contrast enhancement and reflect the extent and severity of myocardial injury after acute reperfused infarction. *Circulation*. 1996; 94:3318–3326.
 24. Weinmann HJ, Laniado M, Mutzel W. Pharmacokinetics of Gd-DTPA-dimeglumine after intravenous injection into healthy volunteers. *Physiol Chem Phys*. 1984;16:167–172.
 25. Steenbergen C, Hill ML, Jennings RB. Volume regulation and plasma membrane injury in aerobic, anaerobic, and ischemic myocardium in vitro. *Circ Res*. 1985;57:864–875.
 26. Jennings RB, Steenbergen C Jr, Kinney RB, Hill ML, Reimer KA. Comparison of the effect of ischaemia and anoxia on the sarcolemma of the dog heart. *Eur Heart J*. 1983;4(suppl H):123–137.
 27. Ramani K, Judd RM, Holly TA, Parrish TB, Rigolin VH, Parker MA, Callahan C, Fitzgerald SW, Bonow RO, Klocke FJ. Contrast magnetic resonance imaging in the assessment of myocardial viability in patients with stable coronary artery disease and left ventricular dysfunction. *Circulation*. 1998;98:2687–2694.
 28. Fedele F, Montesano T, Ferro-Luzzi M, Di Cesare E, Di Renzi P, Scopinaro F, Agati L, Penco M, Serri F, Vitarelli A, Dagianti A. Identification of viable myocardium in patients with chronic coronary artery disease. *Am Heart J*. 1994;128:484–489.
 29. Eichstaedt HW, Felix R, Dougherty FC, Langer M, Rutsch W, Schmutzler H. Magnetic resonance imaging (MRI) in different stages of myocardial infarction using the contrast agent gadolinium-DTPA. *Clin Cardiol*. 1986;9:527–535.
 30. Nishimura T, Kobayashi H, Ohara Y, Yamada N, Haze K, Takamiya M, Hiramori K. Serial assessment of myocardial infarction by using gated MR imaging and Gd-DTPA. *AJR Am J Roentgenol*. 1989;153:715–720.
 31. Van Dijkman PRM, van der Wall EE, de Roos A, Matheijssen NAA, van Rossum AC, Doombos J, van der Laarse A, van Voorthuisen AE, Bruschke AVG. Acute, subacute and chronic myocardial infarction: quantitative analysis of gadolinium-enhanced MR images. *Radiology*. 1991;180:147–151.
 32. Reimer KA, Jennings RB. The changing anatomic reference base of evolving myocardial infarction. *Circulation*. 1979;60:866–876.
 33. Reimer KA, Jennings RB. *Myocardial Ischemia, Hypoxia, and Infarction*. New York, NY: Raven Press Ltd; 1992:1875–1973.